

Spectroscopic studies and Hartree-Fock ab initio calculations of a substituted amide of pyrazine-2-carboxylic acid - $C_{16}H_{18}ClN_3O$

Chacko Yohannan PANICKER^{1,*}, Hema Tresa VARGHESE², Thaha THANSANI¹

¹*Department of Physics, TKM College of Arts and Science, Kollam, Kerala-INDIA*
e-mail: cyphyp@rediffmail.com

²*Department of Physics, Fatima Mata National College, Kollam, Kerala-INDIA*

Received 21.08.2008

A substituted amide of pyrazine-2-carboxylic acid was prepared and the IR spectrum was recorded and analysed. The compound prepared was identified by NMR and mass spectra. The vibrational frequencies of the title compound were computed using the Hartree-Fock level of theory using the 6-31G* basis set and compared with the experimental data. The red shift of the NH stretching frequency indicates weakening of the NH bond. The splitting of the NH stretching bond is due to Davidov coupling between neighbouring units. The first hyperpolarizability, infrared intensities, and Raman activities are reported. Methyl substitution affects all the carbon-nitrogen and carbon-carbon bond lengths of the pyrazine ring of the title compound in comparison with the corresponding bonds of pyrazine. An increase in conjugation enhances the infrared intensity of the carbonyl stretching vibration.

Key Words: Amides of pyrazine carboxylic acid; IR; Hartree-Fock ab initio calculations, hyperpolarizability.

Introduction

Pyrazine and its derivatives form an important class of compounds present in natural flavours and complex organic molecules.¹ Pyrazine is a building block of pterazine and pteridines, and occurs in many compounds with pharmaceutical and flavouring applications. Recent years have seen increased incidence of tuberculosis in both developing and industrialised countries, the widespread emergence of drug-resistant strains, and a deadly synergy with human immunodeficiency virus (HIV).^{2,3} Pyrazinamide is a nicotinamide analogue that has been

*Corresponding author

used for almost 50 years as a first-line drug to treat tuberculosis.⁴ Pyrazinamide is bactericidal to semidormant mycobacteria and reduces total treatment time.⁵ Although the exact biochemical basis of pyrazinamide activity in vivo is not known, under acidic conditions it is thought to be a prodrug of pyrazinoic acid, a compound with antimycobacterial activity.⁶ The finding that pyrazinamide-resistant strains lose amidase (pyrazinamidase or nicotinamidase) activity and the hypothesis that amidase is required to convert pyrazinamide to pyrazinoic acid intracellularly led to the recent synthesis and study of various prodrugs of pyrazinoic acid.⁷ Pyrazine is known to form complexes with carboxylic acids⁸ and nuclear magnetic resonance studies show the 1:1 and 1:2 adducts are present in solution.^{9,10} Furthermore, pyrazine retains its high molecular symmetry and the 2 nitrogen atoms are involved in the complexation. Pyrazines are responsible for the flavour of foodstuffs as diverse as cooked meats, cheese, tea, and coffee. The 2-methylpyrazine is used in flavours in food and tobacco. It is the intermediate of aldinamide and hydragog. In addition, the 2-methylpyrazine is an insecticide, photo medicine and pigment, sensitizer; polymer catalyst of ethylene and other unsaturated compounds, curing agent of epoxy resins, curing agent of halogen polymers, metal chelating agent and separating agent, and brightener of copper plating. Dimethylpyrazines are added to impart or enhance a taste or aroma in food. The 2,3-dimethylpyrazine is found in asparagus, peanuts, coffee and potatoes and is used in gravies, beverages, and candy. The 2,5-dimethylpyrazine is found in beef, blackberries, corn, and grapefruit juice and is used in breakfast cereal. The 2,6-dimethylpyrazine is mainly used to confect the essence of cocoa, coffee, meat, or potato flavor.¹¹ Pyrazine carboxamide is a well known anti-tubercule bacillus drug and some of its complexes are widely used due to their antimycobacterial properties.^{12,13} 2-Chloropyrazine and 2,6-dichloropyrazine are mainly found as medical and agricultural drug intermediates.¹ Billes *et al.*¹⁴ calculated the vibrational frequencies of the 3 parent diazines (pyrazine, pyridazine, and pyrimidine), applying ab initio quantum chemical methods, Molles-Plessett perturbation, and local density function methods. The dynamical pattern of the 2-aminopyrazine-3-carboxylic acid molecule by inelastic and incoherent neutron scattering, Raman spectroscopy, and ab initio calculations is reported by Pawluko \acute{c} *et al.*¹⁵ Various compounds possessing $-NHCO-$ groups, e.g. substituted amides, acyl and thioacyl anilides, benzanilides, and phenyl carbamates, were found to inhibit photosynthetic electron transport.^{16–19} The vibrational spectra of diazines have been extensively studied by several authors.^{14,20–26} However, the literature on methylated derivatives of pyrazine is very scarce.^{11,27–30} Therefore, the vibrational spectroscopic studies of the amides of pyrazine-2-carboxylic acid are additional areas of interest. The synthesis and biological activity of substituted amides of pyrazine-2-carboxylic acids are reported by Dolezal *et al.*³¹ The present study was concerned with the synthesis and analysis of vibrational spectroscopic properties of an amide prepared from substituted pyrazine-2-carboxylic acid.

Experimental

A mixture of acid (i.e. 6-chloropyrazine-2-carboxylic, 5-tert-butylpyrazine-2-carboxylic or 5-tert-butyl-6-chloropyrazine-2-carboxylic acid, 0.05 mol) and thionyl chloride (5.5 mL, 75 mmol) in dry benzene (20 mL) was refluxed for about 1 h. Excess thionyl chloride was removed by repeated evaporation with dry benzene in vacuo. The crude acyl chloride dissolved in dry acetone (50 mL) was added dropwise to a stirred solution of the corresponding substituted aniline (50 mmol) in dry pyridine (50 mL) kept at room temperature. After the addition was complete, stirring was continued for another 30 min. The reaction mixture was then poured into cold water

(200 mL) and the crude amide was collected and recrystallized from aqueous ethanol. Melting points were determined on a Kofler block, and are uncorrected. Elemental analyses were obtained using an EA 1110 CHNS-O CE apparatus (Fisons Instruments S.p.A., Milan, Italy). The IR spectrum (Figure 1) was recorded on a Nicolet Impact 400 spectrometer in KBr pellets. The spectral resolution was 4 cm^{-1} . The standard KBr technique with 0.7 mg per 400 mg KBr was used. The ^1H - and ^{13}C -NMR spectra were measured from CDCl_3 solutions with a Varian Mercury-Vx BB 300 spectrometer operating at 300 MHz. Chemical shifts were recorded as δ values in parts per million (ppm), and were indirectly referenced to tetramethylsilane via the solvent signal (7.26 for ^1H and 77.0 for ^{13}C). Multiplicities are given together with the coupling constants (in Hz). The melting point is 114-115 °C, yield 78% and elemental analyses are: %calculated, %found: C 63.26, 63.15; H 5.97, 5.82; N 13.83, 13.96; Cl 11.67, 11.86. The structure $\text{C}_{16}\text{H}_{18}\text{ClN}_3\text{O}$ (mol. Wt. 303.8) is corroborated by 2D NMR spectroscopy using gHSQC and gHMBC experiments. ^1H -NMR (δ , ppm; J in Hz) 1.56s ($\text{C}(\text{CH}_3)_3$), 2.40s (CH_3), 7.12td ($J=7.41, 1.37, \text{H}5'$), 7.21-7.32m ($\text{H}3'-\text{H}4'$), 8.18-8.13($\text{H}6'$), 9.28s ($\text{H}3$), 9.42s (NH). ^{13}C -NMR (75 MHz, CDCl_3) δ , ppm, J in Hz: 164.5, 159.7, 145.7, 141.3, 140.2, 135.1, 130.5, 128.5, 126.9, 125.3, 121.7, 39.0, 28.2, 17.6.

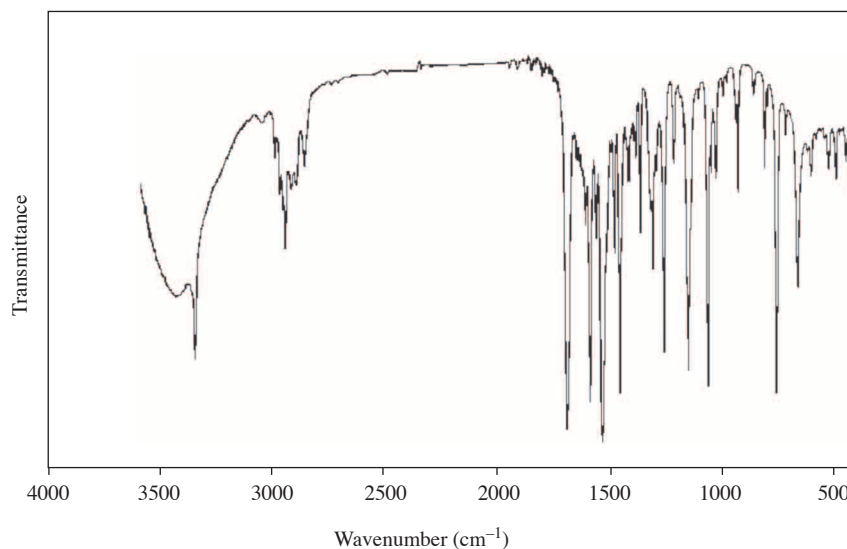


Figure 1. IR spectrum.

Computational details

Calculations of the title compound were carried out with the Gaussian03 program³² using the HF/6-31G* basis set to predict the molecular structure and frequencies. Molecular geometry (Figure 2) was fully optimized by Berny's optimization algorithm using redundant internal coordinates. Harmonic vibrational frequencies were calculated using the analytic second derivatives to confirm the convergence to minimum of the potential surface. The frequency values computed at the Hartree-Fock level contain known systematic errors due to the negligence of electron correlation.³³ We therefore used the scaling factor value of 0.8929 for the HF/6-31G* basis set. The absence of imaginary frequency on the calculated vibrational spectrum confirms that the structure deduced corresponds to minimum energy.

Table. Calculated vibrational frequencies, measured Infrared band positions and assignments.

$\nu_{(HF)}$ (cm ⁻¹)	$\nu_{(IR)}$ (cm ⁻¹)	IR intensity (KM/Mol)	Raman activity (A**4/AMU)	Assignments
3404	3447 sbr 3360 vs	56.17	124.59	ν NH
3043	3040 w	14.93	73.58	ν CH Pz
3029		18.89	221.11	ν CH Ph
3018		31.72	45.77	ν CH Ph
3009		6.57	98.47	ν CH Ph
2999	3000 w	2.61	39.08	ν CH Ph
2971	2978 w	35.14	61.56	ν_{as} Me
2968	2969 m	1.05	10.44	ν_{as} Me
2952	2957 s	32.09	42.31	ν_{as} Me
2939	2940 w	21.98	55.38	ν_{as} Me Ph
2934	2930 w	71.23	125.15	ν_{as} Me
2925		15.59	67.27	ν_{as} Me Ph
2918	2920 w	33.58	88.66	ν_{as} Me
2916	2908 w	15.08	23.53	ν_{as} Me
2878		46.36	257.14	ν_s Me
2872		21.007	125.24	ν_s Me Ph
2868		12.70	25.73	ν_s Me
2867	2860 w	33.90	8.51	ν_s Me
1770	1695 vs	527.22	20.72	ν C=O
1616	1624 w	3.78	17.95	ν Ph
1602	1610 w	12.38	85.05	ν Pz
1587	1593 s	0.28	13.56	ν Ph
1558	1538 vs	13.51	7.34	δ NH
1494		61.82	2.94	ν Pz
1492		10.95	4.05	δ_{as} Me
1479	1484 m	3.13	9.95	ν Ph
1476		4.75	21.58	δ_{as} Me
1467		9.87	4.87	δ_{as} Me Ph
1463		0.20	29.44	δ_{as} Me
1459	1458 s	3.26	20.04	δ_{as} Me Ph
1457		0.34	14.62	δ_{as} Me
1455		0.25	2.03	δ_{as} Me
1452		51.75	2.05	δ_{as} Me
1444		1.34	3.21	ν Ph
1421	1420 w	21.88	8.75	ν Pz

Table. Contunied.

$\nu_{(HF)}$ (cm^{-1})	$\nu_{(IR)}$ (cm^{-1})	IR intensity (KM/Mol)	Raman activity (A**4/AMU)	Assignments
1419		1.42	4.16	δ_s Me
1406	1400 w	2.70	7.45	δ_s Me Ph
1392		5.79	2.08	δ_s Me
1390	1386 m	4.65	1.40	δ_s Me
1334		212.53	4.29	ν Pz
1316	1311 s	267.97	2.73	ν_{as} CC ₃
1272		11.81	5.28	ν Pz
1270	1260 s	16.732	2.55	ν Ph, δ CH Ph
1223	1220 w	19.07	8.31	δ NH
1208		43.07	3.46	ν_{as} CC ₃
1206		2.35	6.36	ρ Me
1187	1180 w	18.91	1.17	ν Pz, δ CH Ph
1183		44.95	0.85	δ CH Ph
1166		6.24	2.70	Ring breath Pz
1147	1150 s	27.07	12.63	δ CH Pz
1102		2.14	4.91	δ CH Ph
1084	1080 w	8.992	3.93	δ CH Ph
1052	1062 s	58.54	5.89	ρ Me
1047	1040 w	3.88	0.54	ρ Me Ph
1032		34.40	4.77	ρ Me
1031		1.20	5.13	ρ Me
1025	1026 w	2.44	14.17	ρ Me, ν Pz
1003		0.04	0.15	γ CH Ph
986		128.11	5.86	ρ Me
977		0.50	2.43	ρ Me Ph
967	960 w	2.24	0.99	γ CH Ph
948		10.85	1.20	γ CH Pz
945	940 w	0.70	0.35	γ CH Ph
911	928 m	0.74	7.47	ν CC
911		0.35	8.59	ν CC
898		9.41	2.36	δ Pz(X)
884		6.05	3.77	δ C=O
858	852 w	17.57	4.23	ν_s CC ₃
810	815 w	6.21	1.26	δ Ph(X)
796	800 w	5.54	7.01	δ Pz
775	780 s	2.96	2.02	γ CH Ph

Table. Contunied.

$\nu_{(HF)}$ (cm^{-1})	$\nu_{(IR)}$ (cm^{-1})	IR intensity (KM/Mol)	Raman activity (A^{*4}/AMU)	Assignments
770		46.41	0.36	$\gamma\text{CH Ph}$
753		10.73	9.37	$\omega\text{C=O}$
720	715 w	32.110	4.33	Ring breath Ph
683		7.05	8.75	γPh
652	663 s	15.89	5.03	$\gamma\text{Ph(X)}$
638.	634 w	10.07	4.52	δCC
596	601 w	14.26	2.45	$\gamma\text{Ph(X)}$
553	560 w	27.28	5.73	ωNH
551		68.50	1.48	$\rho\text{C=O}$
534	538 w	7.12	10.85	δPh
512	515 w	1.13	1.46	$\delta\text{Ph(X)}$
498		12.61	2.53	γPh
486	489 w	3.12	1.27	$\gamma\text{Ph(X)}$
474		5.40	7.02	$\delta\text{Ph(X)}$
454		10.11	1.79	$\delta_{as}\text{CC}_3$
436	440 w	2.62	2.56	νCCl
395	401 w	3.36	2.46	γPz
390		3.02	0.44	$\delta\text{Ph(X)}$
365		1.81	1.39	$\tau\text{C=O}$
347		4.44	1.66	$\delta\text{Ph(X)}$
332		1.79	1.08	$\delta_{as}\text{CC}_3$
316		0.07	0.27	$\delta_s\text{CC}_3$
295		2.24	1.46	δCCl
291		1.79	0.48	ρCC_3
267		1.38	4.69	ρCC_3
234		3.08	3.23	δCN
228		0.08	0.55	τMe
223		1.14	0.92	τMe
190		0.46	1.70	τMe
183		0.38	3.27	γCCl
171		0.28	0.90	$\gamma\text{Pz(X)}$
140		0.78	2.42	δCN
129		0.05	0.48	τCC_3
117		0.45	1.19	$\tau\text{Me Ph}$
79		0.34	1.45	τPz

Table. Contunied.

$\nu_{(HF)}$ (cm^{-1})	$\nu_{(IR)}$ (cm^{-1})	IR intensity (KM/Mol)	Raman activity ($\text{A}^{**4}/\text{AMU}$)	Assignments
60		1.77	1.64	$\tau\text{Me Ph}$
56		0.30	1.11	τPz
38		0.28	4.41	τPh
27		0.26	2.76	τPz
13		0.26	2.94	τPh

ν -stretching; δ -in-plane deformation; γ -out-of-plane deformation; ρ -rocking; -wagging; τ -twisting; ω -wagging; s-strong; b-broad; v-very; w-weak; Me-methyl; Ph-phenyl; Pz- pyrazine; X-substituent sensitive; Me- methyl; subscript : as-asymmetric; s-symmetric.

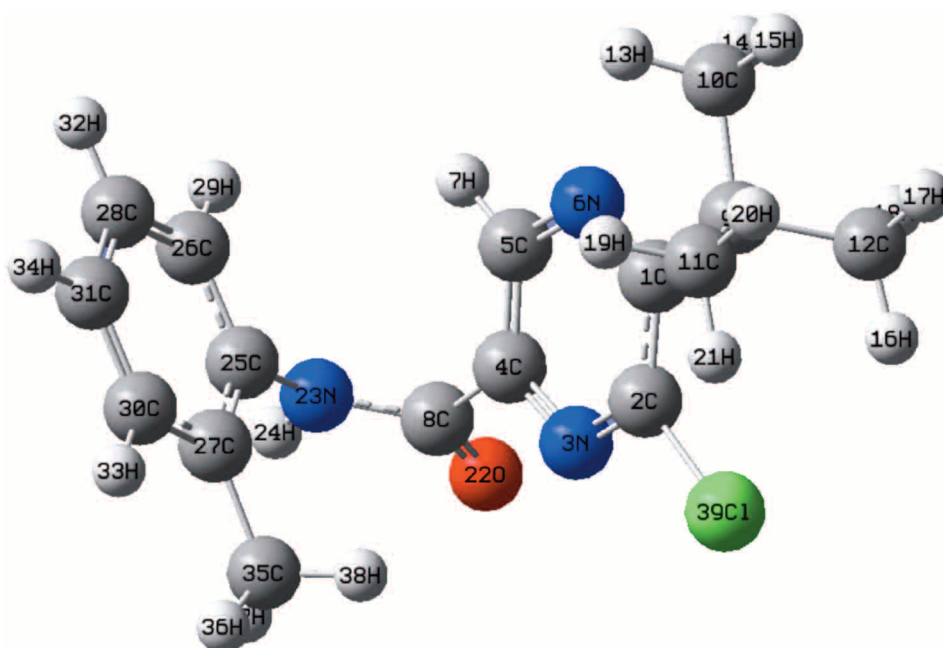


Figure 2. Optimized geometry of the molecule.

Results and discussion

The observed IR bands with their relative intensities and calculated frequencies and assignments are given in the Table.

The N-H stretching vibrations generally give rise to bands^{34,35} at 3500-3300 cm^{-1} . In the present study, the NH stretching band split into a doublet, 3447, 3360 cm^{-1} , in the IR spectrum owing to Davidov coupling between neighbouring units. A similar type of splitting observed in acetanilide^{36,37} and N-methylacetamide³⁸ in the stretching band is also attributed to Davidov splitting. The splitting of about 87 cm^{-1} in the IR spectrum

is due to strong intermolecular hydrogen bonding. Furthermore, the N-H stretching frequency is red shifted by 44 cm^{-1} in the IR spectrum with a strong intensity from the computed frequency, which indicates weakening of the N-H bond resulting in proton transfer to the neighbouring oxygen atom.³⁹ In N-monosubstituted amides, the in-plane bending frequency and the resonance stiffened C-N band stretching frequency fall close together and therefore interact. The CNH vibration where the nitrogen and hydrogen move in opposite directions relative to the carbon atom involves both N-H bend and C-N stretching and absorbs⁴⁰ strongly near 1550 cm^{-1} . This band is very characteristic for mono-substituted amides. The CNH vibration where the N and H atoms move in the same direction relative to the carbon atom gives rise to a weaker band⁴⁰ near 1250 cm^{-1} . In the present case the bands observed at 1538 and 1220 cm^{-1} in the IR spectrum and 1558 and 1223 cm^{-1} (HF) are assigned as CNH bending modes. The out-of-plane NH wag is assigned at 553 cm^{-1} theoretically and at 560 cm^{-1} experimentally.

In the case of 2-aminopyrazine-3-carboxylic acid¹⁵ the vibrational modes of the carboxylic group were assigned to the observed frequencies as follows: torsional C=O 101 cm^{-1} (Raman), 111 cm^{-1} (HF); rocking C=O 537 cm^{-1} (Raman), 571 cm^{-1} (HF); wagging C=O 723 cm^{-1} (Raman), 736 cm^{-1} (HF); bending C=O 912 cm^{-1} (Raman), 886 cm^{-1} (HF); stretching mode C=O 1718 cm^{-1} (Raman), 1786 cm^{-1} (HF). For the title compound the C=O deformation bands are assigned at 884 , 753 , and 551 cm^{-1} theoretically. The carbonyl group vibrations give rise to characteristic bands in the vibrational spectra. The intensity of these bands can increase owing to conjugation or formation of hydrogen bonds. The increase in conjugation, therefore, leads to intensification of IR bands. In the present case the stretching mode of C=O is assigned to the very strong band 1695 cm^{-1} in the IR spectrum and the HF calculations give this mode at 1770 cm^{-1} . The deviation of the calculated value in the HF calculation for this mode can be attributed to the underestimation of the large degree of π -electron delocalization due to conjugation in the molecule.

Although the tertiary butyl substituent can provide 6 methyl asymmetric stretching vibrations, generally only 3 are observed as moderate to strong bands.⁴¹ These vibrations are expected in the region 3010 - 2900 cm^{-1} and most tBu molecules give these $\nu_{as}\text{Me}$ stretching vibrations⁴¹ between 2990 and 2930 cm^{-1} . The methyl symmetric stretching vibrations are active between 2950 and 2850 cm^{-1} . Aromatic molecules usually display these symmetric stretching vibrations⁴¹ between 2915 and 2860 cm^{-1} . In the present case the tBu $\nu_{as}\text{Me}$ stretching vibrations are observed at 2978 , 2969 , 2957 , 2930 , 2920 , and 2908 cm^{-1} in the IR spectrum. The calculated values for these modes are 2971 , 2968 , 2952 , 2934 , 2918 , and 2916 cm^{-1} . The symmetric stretching vibrations of the methyl group are calculated to be at 2878 , 2868 , and 2867 cm^{-1} and only a weak band is observed in the IR spectrum at 2860 cm^{-1} . The methyl asymmetric deformations $\delta_{as}\text{Me}$ absorb⁴¹ between 1495 and 1435 cm^{-1} . Although 3 methyl symmetric bending vibrations are expected often only 2 emerge experimentally. In the present case the band observed at 1386 cm^{-1} in the IR spectrum is assigned as the symmetric deformations of the methyl group. The ab initio calculations give these modes at 1492 , 1476 , 1463 , 1457 , 1455 , and 1452 cm^{-1} and at 1419 , 1392 , and 1390 cm^{-1} as asymmetric and symmetric methyl deformations, respectively, for the title compound.

The $\nu_{as}\text{CC}_3$, $\nu_s\text{CC}_3$ modes are expected in the regions 1235 ± 60 and $800 \pm 90\text{ cm}^{-1}$, respectively⁴¹. For the title compound the band observed at 1311 cm^{-1} in the IR spectrum and 1316 and 1208 cm^{-1} (HF) are assigned as $\nu_{as}\text{CC}_3$ modes. The HF calculations give the symmetric $\nu_s\text{CC}_3$ stretching mode at 858 cm^{-1} and the weak band observed at 852 cm^{-1} in the IR spectrum is assigned as this band. Most of the investigated

molecules display the first methyl rock⁴¹ in the region $1150 \pm 35 \text{ cm}^{-1}$. The other methyl rocking modes are expected in the regions⁴¹ 1035 ± 55 , 990 ± 50 , and $925 \pm 30 \text{ cm}^{-1}$. The HF calculations give these rocking modes of the tBu group at 1206, 1052, 1032, 1031, 1025, and 986 cm^{-1} . Only 2 bands are observed at 1062 and 1026 cm^{-1} in the IR spectrum, as rocking modes of the methyl group. The tBu group gives rise to 5 skeletal deformations absorbing in 3 regions:⁴¹ $\delta_{as} \text{CC}_3$ in 435 ± 85 , $\delta_s \text{CC}_3$ in 335 ± 80 , and ρCC_3 in $300 \pm 80 \text{ cm}^{-1}$. These modes normally produce bands of weak or medium intensity. The highest (lowest) values for $\delta_{as} \text{CC}_3$ are observed⁴¹ around 510 (355) cm^{-1} . Most of the $\delta_{as} \text{CC}_3$ modes have been assigned in the region⁴¹ $435 \pm 65 \text{ cm}^{-1}$. The HF calculations give frequencies at 454, 332, and 316 cm^{-1} as asymmetric and symmetric deformations. The bands at 291 and 267 cm^{-1} (HF) are assigned as the rocking modes of CC_3 . The torsional modes τMe and τCC_3 are expected in the low frequency region.⁴¹

In aromatic compounds the asymmetric stretching vibrations of CH_3 are expected in the range 2905-3000 cm^{-1} and symmetric CH_3 vibrations in the range^{40,41} of 2860-2870 cm^{-1} . The first of these results arises from the asymmetric stretching $\nu_{as} \text{CH}_3$ mode in which 2 C-H bonds of the methyl group are extending while the third one is contracting. The second arises from the symmetrical stretching $\nu_s \text{CH}_3$ in which all 3 of the C-H bonds extend and contract in phase. The asymmetric stretching modes of the methyl group are calculated to be 2939 and 2925 cm^{-1} and the symmetric mode at 2872 cm^{-1} . The band observed at 2940 cm^{-1} in the IR spectrum is assigned as asymmetric mode. Two bending vibrations can occur within a methyl group. The first of these, the symmetrical bending vibration, involves the in-phase bending of the C-H bonds. The second, the asymmetrical bending vibration, involves out-of-phase bending of the C-H bonds. The asymmetrical deformations are expected in the range⁴¹ 1400-1485 cm^{-1} . The calculated values of $\delta_{as} \text{CH}_3$ modes are at 1467 and 1459 cm^{-1} and a band observed at 1458 cm^{-1} in the IR spectrum. In many molecules, the symmetric deformations $\delta_s \text{CH}_3$ appear with an intensity varying from medium to strong and expected in the range⁴¹ $1380 \pm 25 \text{ cm}^{-1}$. The band observed at 1400 cm^{-1} in the IR spectrum is assigned as the $\delta_s \text{CH}_3$ mode. The HF calculations give $\delta_s \text{CH}_3$ mode at 1406 cm^{-1} . Aromatic molecules display a methyl rock⁴¹ in the neighbourhood of 1045 cm^{-1} . The second rock⁴¹ in the region $970 \pm 70 \text{ cm}^{-1}$ is more difficult to find among the C-H out-of-plane deformations. In the present case, these ρCH_3 modes are calculated at 1047 and 977 cm^{-1} . The methyl torsions⁴¹ are often assigned in the region $185 \pm 65 \text{ cm}^{-1}$.

For 2-aminopyrazine-3-carboxylic acid¹⁵ the pyrazine ring stretching modes are observed at 1564, 1536, 1468, 1458, 1360, 1258, and 1083 cm^{-1} (Raman), and 1567, 1565, 1415, 1373, 1231, and 1068 cm^{-1} (ab initio). For pyrazine, the ring stretching modes are reported at 1485, 1411, 1128, and 1065 cm^{-1} (IR); 1579, 1522, and 1015 cm^{-1} (Raman); and 1597, 1543, 1482, 1412, 1140, 1063, and 1009 cm^{-1} theoretically¹. For 2-chloropyrazine the pyrazine ring stretching modes are reported at 1561, 1515, 1198, 1176, 1133, and 1047 cm^{-1} (IR); 1562, 1518, 1197, 1177, 1135, and 1049 cm^{-1} (Raman); and 1563, 1533, 1210, 1116, 1128, and 1042 cm^{-1} (DFT); and for 2,6-dichloropyrazine these vibrations are reported at 1550, 1412, 1230, 1189, 1151, and 1136 cm^{-1} (IR); 1551, 1407, 1172, 1152, and 1131 cm^{-1} (Raman); 1547, 1541, 1407, 1229, 1170, 1167, and 1143 cm^{-1} (DFT);¹ and at 1581, 1525, 1479, 1437, 1166, and 1025 cm^{-1} experimentally for pyrazinamide.⁴² In the present case, the ring stretching modes are observed at 1610, 1420, 1180, and 1026 cm^{-1} in the IR spectrum and the ab initio calculations give these modes at 1602, 1494, 1421, 1334, 1272, 1187, and 1025 cm^{-1} .

The pyrazine CH stretching mode is observed at 3040 cm^{-1} in the IR spectrum and the ab initio calculations give this mode at 3043 cm^{-1} . The CH stretching bands of pyrazine were reported in the range⁴³⁻⁴⁵

3100-3000 cm^{-1} . These νCH bands are observed at 3057, 3070, and 3086 cm^{-1} (IR); 3060, 3070, and 3087 cm^{-1} (Raman); and 3061, 3074, and 3079 cm^{-1} (theoretical) for 2-chloropyrazine; and at 3099 and 3104 cm^{-1} (IR); 3078 and 3103 cm^{-1} (Raman); and 3096 and 3100 cm^{-1} (calculated) for 2,6-dichloropyrazine.¹ Akyuz⁴² reported these νCH bands at 3088, 3066, and 3052 cm^{-1} for pyrazinamide.

For the title compound the out-of-plane deformations γCH vibration of the pyrazine ring is assigned at 948 cm^{-1} theoretically. For pyrazine¹ γCH modes are observed at 790 cm^{-1} in the IR spectrum, 976 and 925 cm^{-1} in the Raman spectrum, and at 985, 974, 930, and 790 cm^{-1} by DFT calculations. The γCH modes are reported at 954, 929, and 844 cm^{-1} (IR); 960, 928, and 847 cm^{-1} (Raman); and 960, 923, and 837 cm^{-1} (theoretical) for 2-chloropyrazine; and at 897 and 875 cm^{-1} (IR); 896 cm^{-1} (Raman); and 919 and 869 cm^{-1} theoretically for 2,6-dichloropyrazine.¹ For 2-aminopyrazine-3-carboxylic acid γCH modes are reported at 1006 and 850 cm^{-1} in the Raman spectrum, 987 and 852 cm^{-1} by HF calculations,¹⁵ and at 988, 954, and 786 cm^{-1} for pyrazinamide.⁴²

The νCCl frequency^{1,30} is reported at $\sim 435 \text{ cm}^{-1}$ and in the present case the band at 440 cm^{-1} in the IR spectrum and 436 cm^{-1} (HF) is assigned as this mode. The deformation bands of CCl are also calculated theoretically at 295 and 183 cm^{-1} , which are in agreement with the reported values.^{1,30}

The C-H in-plane bending modes in 2,6-dichloropyrazine are reported at 1189 and 1151 cm^{-1} in the IR spectrum¹. For 2-chloropyrazine these modes are reported at 1455, 1380, 1280, and 1179 cm^{-1} in the IR spectrum and at 1457, 1390, 1289, and 1167 cm^{-1} theoretically.¹ For pyrazine the δCH modes are observed at 1485, 1413, and 1065 cm^{-1} in the IR spectrum and at 1482, 1412, 1227, and 1063 cm^{-1} theoretically,¹ and for pyrazinamide⁴² at 1305, 1183, and 1054 cm^{-1} . In the present case the ab initio calculations give the C-H in-plane deformation at 1147 and 1150 cm^{-1} in the IR spectrum.

According to Roeges⁴¹ the CH stretching vibrations of the phenyl ring are expected in the region 3120-3000 cm^{-1} . The calculated values for these modes are 3029, 3018, 3009, and 2999 cm^{-1} . Experimentally only a weak band at 3000 cm^{-1} is observed in the IR spectrum. The benzene ring possesses 6 ring stretching vibrations, of which the 4 with the highest frequencies (occurring respectively near 1600, 1580, 1490, and 1440 cm^{-1}) are good group vibrations.⁴¹ The fifth ring stretching vibration is active near $1315 \pm 65 \text{ cm}^{-1}$, a region that overlaps strongly with that of the CH in-plane deformation. The sixth ring stretching vibration or ring breathing mode appears as a weak band near 1000 cm^{-1} in mono and 1,3-di- and 1,3,5-tri-substituted benzenes. In the otherwise substituted benzenes, however, this vibration is substituent sensitive.⁴¹ In the present case, the νPh modes are observed at 1624, 1593, 1484, and 1260 cm^{-1} in the IR spectrum and the HF calculations showed these modes at 1616, 1587, 1479, 1444, and 1270 cm^{-1} . These νPh modes are expected in the region⁴¹ 1625-1275 cm^{-1} . In ortho-disubstitution the ring breathing mode⁴⁶ has 3 frequency intervals according to whether both substituents are heavy, or one of them is heavy while the other is light or both of them are light. In the first case, the interval is 1100-1130 cm^{-1} , in the second case it is 1020-1070 cm^{-1} , while in the third case it is between 630 and 789 cm^{-1} . The band observed at 715 cm^{-1} in the IR spectrum and 720 cm^{-1} (HF) is assigned as the ring breathing mode of the phenyl ring. For 1,2-disubstituted benzenes, the in-plane CH deformations are expected in the range⁴¹ 1250-1300 cm^{-1} and 1170-1000 cm^{-1} . The phenyl CH in-plane deformations δCH are observed at 1260, 1180, and 1080 cm^{-1} in the IR spectrum. The ab initio calculations give these modes at 1270, 1187, 1102, and 1084 cm^{-1} . The aromatic out-of-plane deformations⁴¹ are observed in the range 1005-720 cm^{-1} . These γCH modes are observed at 960, 945, and 780 cm^{-1} in the IR spectrum

and the corresponding calculated values are 1003, 967, 775, and 770 cm^{-1} . According to Roeges,⁴¹ in the case of 1,2-disubstitution only one strong absorption in the region $755 \pm 35 \text{ cm}^{-1}$ is observed and is due to γCH mode. This is confirmed by the presence of a strong γCH at 780 cm^{-1} in the IR spectrum and is supported by the computational result at 775 cm^{-1} .

To best of our knowledge, no X-ray crystallographic data of this molecule have yet been established. However, the theoretical results obtained are comparable with the recently reported structural parameters of similar molecules. In the present case the pyrazine bond lengths of $\text{C}_1\text{-C}_2$, $\text{C}_2\text{-N}_3$, $\text{N}_3\text{-C}_4$, $\text{C}_4\text{-C}_5$, $\text{C}_5\text{-N}_6$, and $\text{N}_6\text{-C}_1$ are 1.4140, 1.2983, 1.3216, 1.3745, 1.3197, and 1.3163 Å, respectively. For a similar derivative, Mary et al.³⁰ reported the corresponding values as 1.3917, 1.2996, 1.3229, 1.3840, 1.322, and 1.3116 Å. Endredi et al.¹¹ reported the bond lengths of $\text{C}_1\text{-C}_2$, $\text{C}_2\text{-N}_3$, $\text{N}_3\text{-C}_4$, $\text{C}_4\text{-C}_5$, and $\text{C}_5\text{-N}_6$ as 1.391, 1.331, 1.331, 1.331, and 1.331 Å for pyrazine; 1.4, 1.327, 1.333, 1.387, and 1.334 Å for 2-methylpyrazine; 1.41, 1.331, 1.33, 1.385, and 1.331 Å for 2,3-dimethylpyrazine; 1.396, 1.327, 1.335, 1.396, and 1.335 Å for 2,5-dimethylpyrazine; and 1.399, 1.326, 1.332, 1.399, and 1.332 Å for 2,6-dimethylpyrazine. For 2-aminopyrazine-3-carboxylic acid¹ and for a similar substituted amide of pyrazine³⁰, the bond lengths of $\text{C}_8\text{-O}_{22}$, $\text{C}_4\text{-C}_8$, $\text{C}_4\text{-N}_3$, and $\text{C}_4\text{-C}_5$ are 1.212, 1.479, 1.333, and 1.479 Å, and 1.2003, 1.5099, 1.3229, and 1.384 Å, respectively. In the present case, the corresponding values are 1.1943, 1.5097, 1.3216, and 1.3745 Å, respectively. The CN bond lengths in the pyrazine ring of the title compound $\text{C}_2\text{-N}_3$ 1.2983, $\text{C}_4\text{-N}_3$ 1.3216, $\text{C}_1\text{-N}_6$ 1.3163, and $\text{C}_5\text{-N}_6$ 1.3197 Å are much shorter than the normal C-N single bond that is referred to 1.49 Å. The same results are shown for the bond lengths of the 2 C-C bonds, $\text{C}_1\text{-C}_2$ 1.4140 and $\text{C}_4\text{-C}_5$ 1.3745 Å in the pyrazine ring and are also smaller than that of the normal C-C single bond of 1.54 Å.⁴⁷ The C-N bond lengths $\text{C}_8\text{-N}_{23}$ 1.3621 and $\text{C}_{25}\text{-N}_{23}$ 1.4303 Å are also shorter than the normal C-N single bond of 1.49 Å, which confirms this bond to have some character of a double or conjugated bond.⁴⁸ The $\text{N}_{23}\text{-H}_{24}$ bond is found to be 0.9994 Å, which is around the normal NH bond of 1.01 Å⁴⁷. The CCl bond length in the present case is 1.7422 Å, which is in agreement with the previous reported value^{1,30}. The substitution of chlorine in the pyrazine ring shortens the $\text{C}_2\text{-N}_3$ bond length and elongates the $\text{C}_2\text{-C}_1$ bond length, in comparison with the other CN and CC bond lengths of the pyrazine ring. Chlorine is highly electronegative and tries to obtain additional electron density. It attempts to draw it from the neighbouring atoms, which move closer together in order to share the remaining electrons more easily as a result. Due to this the bond angle $\text{A}(1,2,3)$ is found to be 122.9° and the exocyclic angles $\text{A}(3,2,39)$ and $\text{A}(1,2,39)$ become 113.8 and 123.3° , respectively.

Due to $\text{C}(\text{CH}_3)_3$ substitution in the pyrazine ring the $\text{C}_1\text{-C}_2$ bond length is greater than the $\text{C}_4\text{-C}_5$ bond length. The +I>-M effect of the methyl substituent affects all the C-N and C-C bond lengths of the pyrazine ring of the title compound in comparison with the corresponding bonds of pyrazine.¹¹ At the N_{23} position, the angle of $\text{C}_8\text{-N}_{23}\text{-H}_{24}$ is 112.3° , $\text{C}_{25}\text{-N}_{23}\text{-H}_{24}$ is 117.1° , and $\text{C}_8\text{-N}_{23}\text{-C}_{25}$ is 127.4° . This asymmetry of the angles at the N_{23} position indicates³⁹ the weakening of the $\text{N}_{23}\text{-H}_{24}$ bond, resulting in proton transfer to the oxygen atom O_{22} . At the C_{27} position, the angle $\text{C}_{25}\text{-C}_{27}\text{-C}_{30}$ is reduced by 2.2° and that of $\text{C}_{25}\text{-C}_{27}\text{-C}_{35}$ is increased by 1.7° from 120° , which shows the repulsive interaction between the methyl group and NH group. At the C_1 position of the pyrazine ring, there is asymmetry between the angles $\text{C}_2\text{-C}_1\text{-C}_9$ and $\text{N}_6\text{-C}_1\text{-C}_9$ due to the steric hindrance between H_8 and the tBu group.

The first hyperpolarizability of this novel molecular system is calculated using the HF/6-31G* basis set,

based on the finite field approach. In the presence of an applied electric field, the energy of a system is a function of the electric field. First hyperpolarizability is a third rank tensor that can be described by a $3 \times 3 \times 3$ matrix. The 27 components of the 3D matrix can be reduced to 10 components due to the Kleinman symmetry.⁴⁸ The components of β are defined as the coefficients in the Taylor series expansion of the energy in the external electric field. When the electric field is weak and homogeneous, this expansion becomes

$$E = E_0 - \sum_i \mu_i F^i - \frac{1}{2} \sum_{ij} \alpha_{ij} F^i F^j - \frac{1}{6} \sum_{ijk} \beta_{ijk} F^i F^j F^k - \frac{1}{24} \sum_{ijkl} \gamma_{ijkl} F^i F^j F^k F^l + \dots$$

where E_0 is the energy of the unperturbed molecule, F^i is the field at the origin, μ_i , α_{ij} , β_{ijk} , and γ_{ijkl} are the components of dipole moment, polarizability, the first hyper polarizabilities, and second hyperpolarizabilities, respectively. The calculated first hyperpolarizability of the title compound is 1.228×10^{-30} esu, which is comparable with the reported values of similar derivatives⁴⁹ and experimental evaluation of these data is not readily available. We conclude that the title compound is an attractive subject for future studies of NLO properties.

Acknowledgements

The authors thank the Kerala State Council for Science, Technology and Environment, Government of Kerala, India, for financial support.

References

1. Endredi, H.; Billes, F.; Holly, S. *J. Mol. Struct. Theochem.* **2003**, *633*, 73-82.
2. Raviglione, M. C.; Dye, C.; Smidt, S.; Kochi, A. *Lancet.* **1997**, *35*, 624-629.
3. Houston, S.; Fanny, A. *Drugs* **1996**, *48*, 689-696.
4. Snider, D. E.; Castro, K. G. *New Engl. J. Med.* **1998**, *38*, 1689-1690.
5. Mitchison, D. A. *Natur. Med.* **1996**, *2*, 635-636.
6. Cynanon, M. H.; Klemens, S. P.; Chou, T. S.; Gimi, R. H.; Welch, J. T. *J. Med. Chem.* **1992**, *35*, 1212-1215.
7. Bergmann, K. E.; Cynanon, M. H.; Welch, J. T. *J. Med. Chem.* **1996**, *39*, 3394-3400.
8. Belabbes, Y.; Lautid, A. *Vib. Spectrosc.* **1995**, *9*, 131-137.
9. Fujiwara, H.; Yoshida, N.; Ilkenoue, T. *Bull. Chem. Soc. Jpn.* **1975**, *48*, 1970-1976.
10. Rebek, J.; Nemeth, D. *J. Am. Chem. Soc.* **1986**, *108*, 5637-5638.
11. Endredi, H.; Billes, F.; Keresztury, G. *J. Mol. Struct. Theochem.* **2004**, *677*, 211-225.
12. 12. Katzung, B. G. *Basic and Clinical Pharmacology*, fourth ed. Prentice Hall, London, 1989.
13. Opletalova, V.; Hartl, J.; Patel, A.; Palat Jr. K.; Buchta, V. *Il Farmaco.* **2002**, *57*, 135-144.
14. Billes, F.; Mikosch, H.; Holly, S. *J. Mol. Struct. Theochem.* **1998**, *423*, 225-234.
15. Pawlukoje, A.; Natkaniec, I.; Makrski, Z.; Leciejewicz, J. *J. Mol. Struct.* **2000**, *516*, 7-14.

16. Good, N. E. *Plant. Physiol.* **1961**, *36*, 788-803.
17. Kralova, K.; Sersen, F.; Cizmarik, J. *Chem. Pap.* **1992**, *46*, 266-268.
18. Kralova, K.; Sersen, F.; Miletin, M.; Hartal, J. *Chem. Pap.* **1998**, *52*, 52-55.
19. Kralova, K.; Sersen, F.; Kubicova, L.; Waisser, K. *Chem. Pap.* **1999**, *53*, 328-331.
20. Arenas, J. F.; Wolley, M. S.; Lopez-Tocon, I.; Otero, J. C. *J. Chem. Phys.* **2000**, *112*, 7669-7683.
21. Moskovits, M.; DiLella, D. P.; Maynard, K. J. *Langmuir.* **1988**, *4*, 67-76.
22. Brolo, A. G.; Irish, D. E. *Z. Naturforsch.* **1995**, *50*, 274-282.
23. Martin, J. M. L.; Van Alsenoy, C. *J. Phys. Chem.* **1996**, *10*, 6793-6983.
24. Boese, A. D.; Marin, J. M. L. *J. Phys. Chem.* **2004**, *108A*, 3085-3096.
25. Barone, V. *J. Phys. Chem.* **2004**, *108A*, 4146-4150.
26. Breda, S.; Reva, I. D.; Lapinski, L.; Nowak, M. J.; Fausto, R. *J. Mol. Struct.* **2006**, *786*, 193-206.
27. Arenas, J. F.; Lopez-Tocon, I.; Otero, J. C.; Marcos, J. L. *Vib. Spectrosc.* **1999**, *19*, 213-221.
28. Arenas, J. F.; Centeno, S. P.; Lopez-Tocon, I.; Otero, J. C. *J. Mol. Struct.* **2005**, *744*, 289-293.
29. Centeno, S. P.; Lopez-Tocon, I.; Arenas, J. F.; Otero, J. C. *J. Mol. Struct.* **2007**, *834*, 567-571.
30. Mary, Y. S.; Varghese, H. T.; Panicker, C. Y.; Dolezal, M. *Spectrochim. Acta* doi: 10.1016/j.saa.2007.12.055.
31. Dolezal, M.; Miletin, M.; Kunes, J.; Kralova, K. *Molecules* **2002**, *7*, 363-373.
32. Frisch, M. J.; Trucks, G. W.; Schlegel, H. B.; Scuseria, G. E.; Robb, M. A.; Cheeseman, J. R.; Montgomery, Jr., J. A.; Vreven, T.; Kudin, K. N.; Burant, J. C.; Millam, J. M.; Iyengar, S. S.; Tomasi, J.; Barone, V.; Mennucci, B.; Cossi, M.; Scalmani, G.; Rega, N.; Petersson, G. A.; Nakatsuji, H.; Hada, M.; Ehara, M.; Toyota, K.; Fukuda, R.; Hasegawa, J.; Ishida, M.; Nakajima, T.; Honda, Y.; Kitao, O.; Nakai, H.; Klene, M.; Li, X.; Knox, J. E.; Hratchian, H. P.; Cross, J. B.; Adamo, C.; Jaramillo, J.; Gomperts, R.; Stratmann, R. E.; Yazyev, O.; Austin, A. J.; Cammi, R.; Pomelli, C.; Ochterski, J. W.; Ayala, P. Y.; Morokuma, K.; Voth, G. A.; Salvador, P.; Dannenberg, J. J.; Zakrzewski, V. G.; Dapprich, S.; Daniels, A. D.; Strain, M. C.; Farkas, O.; Malick, D. K.; Rabuck, A. D.; Raghavachari, K.; Foresman, J. B.; Ortiz, J. V.; Cui, Q.; Baboul, A. G.; Clifford, S.; Cioslowski, J.; Stefanov, B. B.; Liu, G.; Liashenko, A.; Piskorz, P.; Komaromi, I.; Martin, R. L.; Fox, D. J.; Keith, T.; Al-Laham, M. A.; Peng, C. Y.; Nanayakkara, A.; Challacombe, M.; Gill, P. M. W.; Johnson, B.; Chen, W.; Wong, M. W.; Gonzalez, C.; Pople, J. A. *Gaussian 03, Revision C.02*, Gaussian, Inc., Wallingford CT, 2004.
33. Foresman, J. B. in *Exploring Chemistry with Electronic Structure Methods: A Guide to Using Gaussian*, Eds.; Frisch, E. (Ed.), Gaussian, Pittsburgh, PA, 1996.
34. Spire, A.; Barthes, M.; Kallouai, H.; DeNunzio, G. *Physics* **2000**, *D137*, 392-396.
35. Bellamy, L. J. *The IR Spectra of Complex Molecules*, John Wiley and Sons, New York, 1975.
36. Edler, J.; Pfister, R.; Pouthier, V.; Falvo, C.; Hamm, P. *Phys. Rev. Lett.* **2004**, *93*, 106405-106408.
37. Edler, J.; Hamm, P.; Scott, A. C. *Phys. Rev. Lett.* **2002**, *88*, 067403-067406.
38. Edler, J.; Hamm, P. *Phys. Rev.* **2004**, *B69*, 214301-214308.
39. Barthes, M.; DeNunzio, G.; Ribert, G. *Synth. Met.* **1996**, *76*, 337-340.
40. Colthup, N. B.; Daly, L. H.; Wiberly, S. E. *Introduction to Infrared and Raman Spectroscopy*, second ed., Academic Press, New York, 1985.

41. Roeges, N. P. G. *A Guide to the Complete Interpretation of Infrared Spectra of Organic Structures*, Wiley, New York, 1994.
42. Akyuz, S. *J. Mol. Struct.* **2003**, *651*, 541-545.
43. Schettino, V.; Sbrana, G.; Righini, R. *Chem. Phys. Lett.* **1972**, *13*, 284-285.
44. Sbrana, G.; Schettino, V.; Righini, R. *J. Chem. Phys.* **1973**, *59*, 2441-2450.
45. Arenas, J. F.; Navarrete, I. T. L.; Otero, J. C.; Marcos, J. I.; Cardenate, A. *J. Chem. Soc. Faraday Trans. 2*, **1985**, *81*, 405-416.
46. Varsanyi, G. *Assignments of Vibrational Spectra of Seven Hundred Benzene Derivatives*, Wiley New York 1974.
47. He, W.; Zhon, G.; Li, J.; Tian, A. *J. Mol. Struct. Theochem.* **2004**, *668*, 201-208.
48. Kleinman, D. A. *Phys. Rev.* **1962**, *126*, 1977-1979.
49. Bakalova, S. M.; Santos, A. G.; Timcheva, I.; Kaneti, J.; Filipova, I. L.; Dabrikov, G. M.; Dimitrov, V. D. *J. Mol. Struct. Theochem.* **2004**, *710*, 229-234.